Fabrication and characterization of a TiO_2 nanoparticles polypropylene membrane: application in indoor air quality maintenance

A. S. Favas[a,*], B. Bavanish[b],
[a]*Research Scholar, Mechanical Engineering, Noorul Islam Centre for Higher Education, Kumarcoil -629180, Tamilnadu, India*
[b]*Associate Professor, Fire Technology and Safety Engineering, Noorul Islam Centre for Higher Education, Kumarcoil -629180, Tamilnadu, India*

The production of innovative materials with improved features applicable in many domains is a key application of nanotechnology with far-reaching implications for modern society. Nanoparticle-based polymer composites are quickly becoming one of the most promising new materials, with potential uses spanning the chemical, physical, and biological sciences as well as engineering. Application of nanoparticle-based polymer composites for indoor air quality maintenance was discussed, as were their production, hybrid functionalization, and feasible synthesis procedures (filter membrane). The batch foaming procedure has been used to create foam from the thermoplastic polymer polypropylene (PP). Foaming is a blown process, where carbon dioxide is utilised as the blowing agent. Nanoparticles of titanium oxide (nano TiO_2) are also used for reinforcement. Scanning electron microscopy (SEM) was utilised to investigate the NTPMs' surface morphology, while other physio-chemical characteristics were investigated by means of various analytical methods, including Fourier transform infrared spectroscopy (FTIR), X-ray diffraction (XRD), and thermo-gravimetric analysis (TGA). The adsorption isotherm and kinetics of water vapours were analysed to get insight into the water vapour adsorption characteristics of the NTPMs. The kinetics of adsorption pointed to a combination of intraparticle diffusion and liquid field driving processes for the transport of water vapours. Because of their high dehumidification effectiveness, synthetic NTPMs have the potential to replace many of the currently used traditional solid desiccant materials.

(Received April 28, 2023; Accepted July 17, 2023)

Keywords: Polypropylene foam, TiO_2 nano powders, Dehumidification, Adsorption kinetics

1. Introduction

Desiccant materials are a large category that includes both solid and liquid hygroscopic substances used to absorb water vapour from humidity. For example, lithium chloride (LiCl) and calcium chloride ($CaCl_2$) are two examples of hygroscopic salts that are classified as liquid desiccants[1]. However, these hygroscopic salts also have a deliquescence feature, meaning that they dissolve in the adsorbed water to form crystalline hydrates[2]. This is in contrast to their relatively high-water vapours adsorption capabilities. As a result, these materials are very challenging to work with and have few potential uses. Materials including molecular sieves, silica gel, activated carbon, metal organic frameworks (MoF's), clays, zeolites, and polymer desiccants make up the other kind of desiccant[3]. Solid desiccants are less effective in removing moisture from the air than their liquid counterparts, but they have the advantages of being more stable and less hazardous to work with. Despite their relatively poor adsorption capabilities, solid desiccants have found widespread usage in a variety of commercial and domestic settings. The packing industry and the HVAC sector rely heavily on solid desiccants[4]. Pharmaceutical, electrical, shoe, and textile manufacturers all rely on solid desiccant materials to keep their goods safe from damage caused by humid air.

* Corresponding author: favasphd@gmail.com
https://doi.org/10.15251/JOBM.2023.153.81

Molecular sieves, clays, and silica gel are the most widely used solid desiccant materials in the packaging industry; however, they have low dehumidification efficiencies at a given humidity level and a high desorption temperature, both of which necessitate a great deal of energy to regenerate the desiccants[5]. Polymeric materials were studied as a potential replacement for traditional solid desiccants. However, their dehumidification efficiency is often subpar due to their complicated adsorption process[6]. Additionally, composites of various polymers containing hygroscopic salts were produced to improve their adsorption capacities[7]. Using the polymer as a matrix to prevent the deliquescent salt from dissolving was a primary concern in the development of these composites. Most of the time, polymeric materials were merely utilised as a matrix to prevent the dissolution of deliquescent salts and did not significantly contribute to the adsorption process. The high regeneration temperatures required by these polymer composites is their primary drawback. Thus, innovative polymer materials with enhanced adsorption capabilities and low regeneration temperature should be developed to enhance the efficacy of these solid desiccants.

Lightweight conductive PP foams with reduced nanoparticle content and improved electrical and electromagnetic interference (EMI) shielding capabilities were made possible by the introduction and orientation of nanocarbon elements[8]. To sum up, nanofillers not only have the potential to improve PP cell nucleation, but also to impart PP foams with novel and superior characteristics. Titanium dioxide (TiO_2), zinc oxide (ZnO), and germanium dioxide (GeO_2) are examples of nanometric metal oxide semiconductors used to enhance the chemical and thermal durability of inorganic UV absorbers[9]. Since rutile TiO_2 effectively absorbs UV radiation and has a more stable crystal structure and a wider absorption wavelength area than anatase type TiO2, it is commonly utilised as a UV shielding agent 25. Rutile TiO_2 is photocatalytic because the electrons in the material are excited and transferred when the material is exposed to UV light; the resulting electron-hole pairs have a redox capacity and decompose organic molecules in their vicinity[10]. Therefore, in this study, a polypropylene (PP) and titanium dioxide (TiO_2) nanofiller based super-porous membrane (NTPM) was developed to absorb water vapours from humid air. The NTPMs have a highly porous structure with linked capillary channels. The current study synthesised NTPMs using the gas foaming and blowing process and analysed their capacity to absorb water vapour from humid air at various temperatures. At 85% relative humidity and 25°C, the synthesised NTPMs had a dehumidification capacity of 0.578 gw/gads without the addition of any deliquescent salt. Adsorption isotherm and adsorption kinetics studies were performed to further understand the remarkable dehumidification effectiveness of the synthesised NTPMs.

2. Experimental

2.1. Materials

Polypropylene (PP) and Titanium dioxide nanopowder (TiO_2 rutile <100 nm particle size) was purchased from Sigma Aldrich and were used as received. Carbon dioxide (CO_2) with a purity of 99.9% was supplied by Audhyogik Special Gases, Uttar Pradesh, India.

2.2. Preparation of Nano-TiO_2 polypropylene Membrane (NTPM)

NTPM were produced by melting PP and nano 5 Wt.% of TiO_2 in a mixer at 200^0C with a rotor speed of 10 rpm for one minute, followed by 50 rpm for six minutes. With the use of a flat vulcanizer at a temperature of 200^0C, the NTPM was further squeezed into sheets 1 mm thick. The NTPM samples were preheated for 4 minutes, then held at 8.5 MPa for 3 minutes, before being cooled by flowing water at the same pressure. When making batch foam, the square sheets (1 X 1 cm2 each) were employed. Using supercritical carbon dioxide as a physical blowing agent[11], foamed NTPM were produced in an autoclave. Low-pressure carbon dioxide (CO_2) was continuously pumped into the autoclave for around 3 minutes to displace the air within and sterilise the NTPM samples. The vessel was then placed in an oil bath at 165^0C and 20 MPa of pressure to maintain the NTPM samples saturated for 2 hours. The vessel was then submerged in cold water to quench the foam structure and depressurized at a rate of around 10 MPa/s.

2.3. Characterization

The FT-IR spectra was reported between the wavenumbers of 4000−400 cm^{-1} using the SHIMADZU FTIR 8400S spectrometer by mixing the samples evenly with KBr. At ambient temperature, the XRD diffractograms of NTPM was analyzed using a diffractometer called a Rigaku Mini Flex 600s. This instrument used an X-ray tube with a copper anode to produce Cu-Kα radiation at a setting of 30 kV and mA. Scanning electron microscopy was used in order to investigate the nanoparticles of titanium's dispersion inside the polymer matrix (SEM, Jeol JSM-7600 F). A thermogravimetric analyzer (TGA) Model Perkin Elmer Pyris was used for the process of performing the thermogravimetric analysis on the samples. In the presence of nitrogen, samples of nanocomposites were subjected to a temperature increase from 25^0C to 550^0C at a rate of 20^0C per minute.

2.4. Water vapour adsorption

The ability of the synthesized NTPM to adsorb water vapors from the moist air was investigated using adsorption chamber. The samples used in the test were 1 X 1 cm^2 and were dried in an oven until they reached a consistent weight. The initial weight, denoted by (WI), and the final weight, denoted by (WF), are as follows: The moisture absorption was performed in a chamber with a relative humidity of 85% and a temperature of 25^0C. The final weight (WF) of the sample is determined by reweighing it after every 30 minutes. According to the findings of a prior investigation, the percentage of moisture absorption was computed using the equation shown below[12].

$$\%\ of\ Moisture\ Absorption = \frac{W_F - W_I}{W_I}\ X\ 100 \quad (1)$$

Various conditions, including temperature (25, 35, 45, and 55 °C) and relative humidity (20-85%), were tested to determine the adsorption isotherm for water vapours. At 25°C and 85% relative humidity, NTPM was tested for its adsorption kinetics. Samples were weighed before and after being exposed to humid air, at predetermined intervals. After being fully hydrated, NTPM was then regenerated at 60°C for use in another adsorption cycle to test its reusability. Fifteen cycles of adsorption and regeneration were performed on NTPM that had been hydrated.

3. Result and discussion

3.1. Characterization

Figure 1 displays the diffraction patterns of NTPM made from poly-P and including nano TiO_2. Titanium nanoparticles were detected as strong peaks in the polymer findings, suggesting the presence of nano fillers[13].

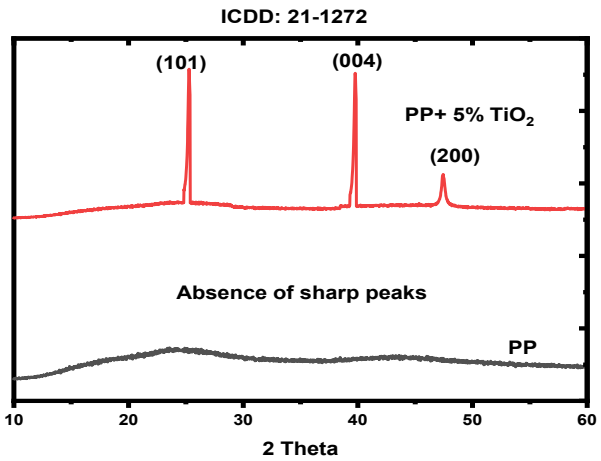

Fig. 1. XRD patterns of NTPM and PP.

X-ray diffraction patterns reveal that the titanium nanoparticles have main peaks at 25.27^0 (101), 37.91^0 (004), and 47.90^0 (200). All the lines in this design may be indexed by the PDF number 21-1272 that stands for titanium[14].

The NTPM's FTIR spectra are shown in Figure.2. It was suggested that TiO_2 nanopowders were hydrophilic by the absorption peaks at 3433 cm^{-1} and 1708 cm^{-1} in the TiO_2 spectra, which correspond to the stretching and bending vibration of the surface hydroxyl (-OH) groups. The fact that NTPM revealed a peak at 684 and 752 cm^{-1}, which is consistent with metal oxides, indicates that titanium oxide nanofillers are present in the polypropylene matrix[15].

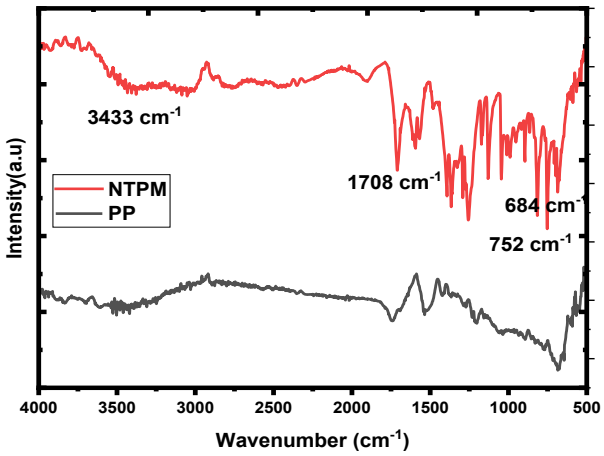

Fig. 2. FTIR spectrum of NTPM and PP.

The thermal stability of NTPM was evaluated using thermogravimetric analysis (TGA). Figure 3 displays the TGA curves for NTPM. Figure 3 depicts the single process involved in the thermo-oxidative breakdown of polymer nanocomposites. The first sign of PP degradation, in the form of a 1% weight loss, occurs at 348°C, 240°C, and the process continues up to 472°C, 330°C. As the TGA curve shows, the mass does not change after hitting 472°C and 330°C. When TiO_2 nano powders content was added to polypropylene[16], the breakdown peak shifted to higher temperatures (up to 377°C, 330°C). Therefore, the melting point of NTPM with 5% TiO_2 is 321°C,730°C. Clearly, the heat resistance of the ready-made NTPM is drastically altered by the incorporation of TiO_2 nano powders into the polypropylene matrix.

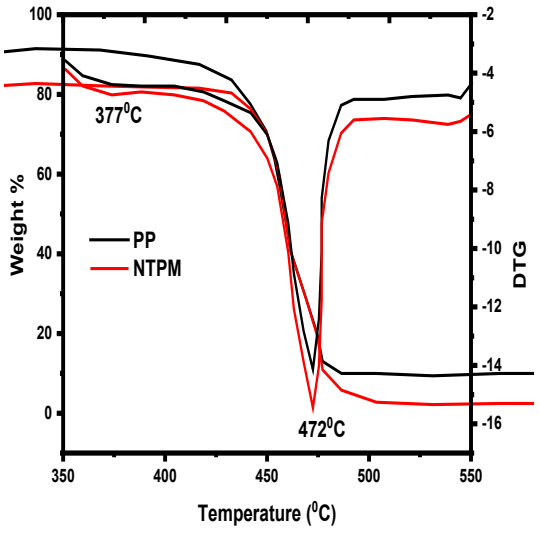

Fig. 3. TGA-DTG spectrum of NTPM and PP.

The incorporation of TiO_2 nano powders into polypropylene also improves the material's resistance to heat. It is generally accepted that the porous architecture of NTPM is largely responsible for their remarkable capacity to absorb water. Therefore, the SEM was used to look at the NTPM's surface morphology and pore structure (Figure.4). The NTPM has a porous macrostructure and a smooth texture, and its surface is covered with pores that branch out in different directions to form capillary channels. The highly interconnected nature of these capillary channels is what allowed for such rapid kinetics and high-water absorption capacity[17].

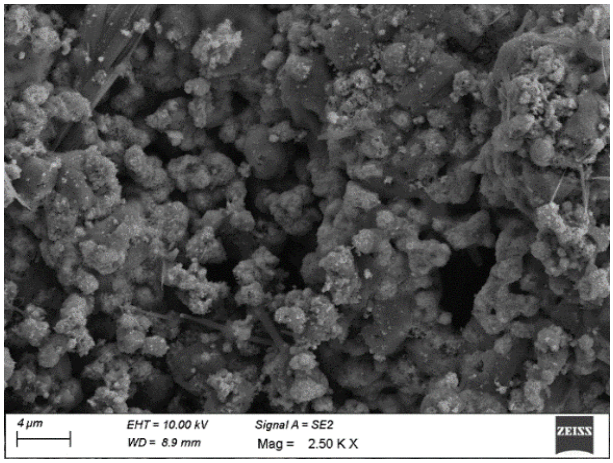

Fig. 4. SEM image of NTPM.

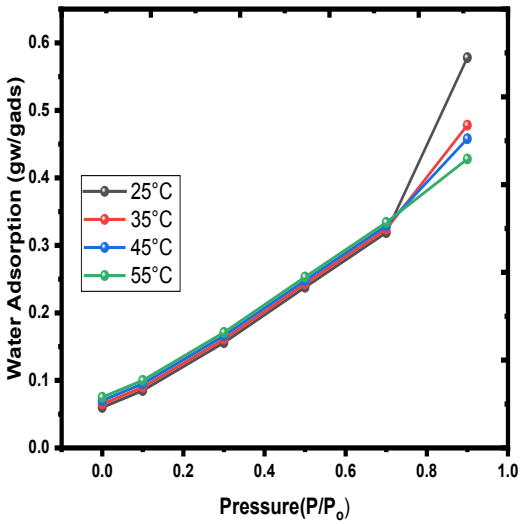

Fig. 5. Adsorption isotherm at different temperatures for the NTPM in the relative humidity range of 20 to 85%.

3.2. Adsorption isotherm

At temperatures of 25, 35, 45, and 55 °C, the isotherms for the adsorption of water vapours onto NTPM were analysed for relative humidity ranging from 20% to 85%. (Figure.5). Water molecules are typically adsorbed by capillary condensation using the linked channels of pores present in the structure, and the adsorption isotherm was shown to match the type-III adsorption isotherm over a wide temperature range[18]. After adsorption, most of the water molecules in this form of adsorbent are present as free water due to their entrapment in the cavities. Water is adsorbed onto an adsorbent, but only a tiny percentage of that water binds to functional groups on the surface of the adsorbent[19]. SEM images (Figure.4) demonstrated the

existence of linked capillary channels, further supporting the existence of a type-III adsorption isotherm for NTPM. When looking at the isotherm pattern of NTPM, two primary sections stand out: the first, where the adsorption capacity was low and it existed at relative humidity less than 50%, and the second, where the adsorption capacity was extremely high and it existed when the relative humidity was between 50 and 85%. Maximum adsorption capacity at 25 °C was only 0.06 gw/gads in the first section (relative humidity 50%), where water molecules were mostly bound to the surface functional groups of NTPM. Because water molecules' partial pressure is insufficient to penetrate the polymer structure, the adsorption capacity was rather low in this area. This meant that the capillary condensation process[20], by which water molecules would normally penetrate the interior polymer structure, was not possible.

Table 1. The water vapors adsorption isotherm on NTPM.

Parameter	**Temperature °C**				**Model**
	25	**35**	**45**	**55**	
k_F (L/mg)$^{1/n}$ (mg/g)	1.28	0.72	0.485	0.354	Freundlich
n	0.15	0.2	0.212	0.22	
AIC	-51.34	-54.89	-58.12	-64.37	
BIC	-55.14	-58.27	-63.98	-68.52	
R^2	0.985	0.954	0.948	0.961	
q_m (g_w/g_{ads})	0.578	0.368	0.257	0.198	BET
c	1.22	1.83	1.15	2.36	
AIC	-81.34	-84.89	-88.12	-94.37	
BIC	-95.14	-98.27	-103.98	-108.52	
R^2	0.989	0.995	0.999	0.989	

The NTPM's highest adsorption capacity was 0.578 gw/gads at 25°C and 85% relative humidity, which was seen in the second adsorption area (relative humidity between 50 and 85%). Higher adsorption capacity in the second area revealed that the hydrophilic character of NTPM increased with increasing relative humidity and that most of the water molecules were adsorbed through capillary condensation process and existed as free water molecules. Since the partial pressure of water molecules increases with increasing relative humidity, allowing for deeper penetration into the interior structure through capillary condensation, the adsorption capacity was particularly high in this region[21]. For all temperatures examined, the adsorption isotherm slope was not steep in the lower relative humidity regions, indicating that NTPM lacked high affinity for water vapours and exhibited lower adsorption capacities than conventional adsorbents like zeolites(Ze) and silica-gel, which typically exhibit type-I adsorption isotherm[22].

On the other hand, when relative humidity rose, NTPM's ability to absorb water vapours rose to levels well beyond those of most traditional solid desiccant materials. The endothermic nature of the adsorption of water vapours on NTPM was further supported by the fact that its adsorption capability steadily reduced as the temperature was increased. Non-linear forms of many isotherm models, including the Brunauer-Emmett-Teller (BET) (Figure.6b) and the Freundlich (Figure.6a), were used to match the adsorption isotherm data[23]. The Akaike Information Criterion (AIC), the Bayesian Information Criterion, and other parameters' values all had an impact on how strongly the experimental data and the BET isotherm model correlated. (BIC), and the correlation coefficient (R2) (Table.1). The BET isotherm model provided a good match for the adsorption isotherm data (Figure.6b). This model can be used to explain multi-layer adsorption isotherms that follow type II and type III isotherms. As a result, the application of the BET isotherm suggested a multilayer sorption process and offered greater support for the type-III adsorption isotherm. Furthermore, based on the value of monolayer moisture content (qm) obtained using the BET model, which represents the amount of water molecules attached to the adsorbent's ionic and polar surface functional groups via different binding forces, the amount of water vapours adsorbed on the surface of NTPM was predicted to decrease with increasing temperature.

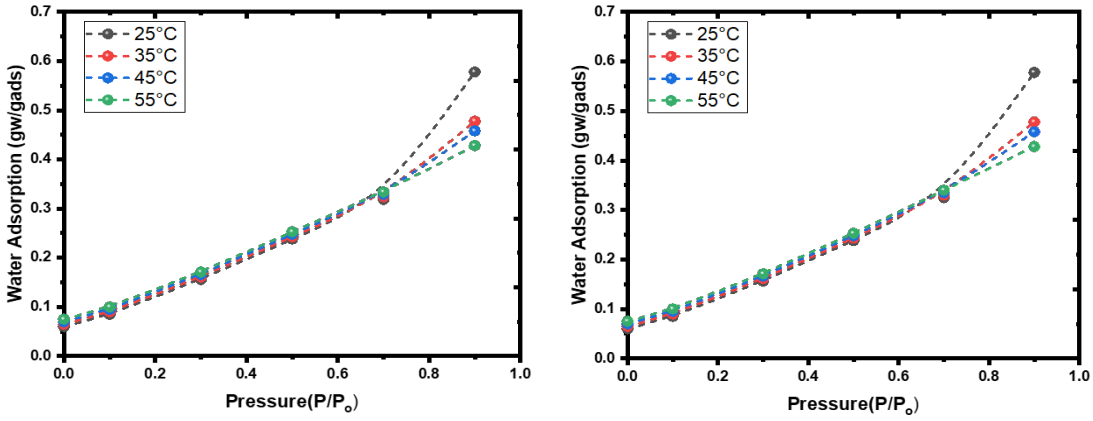

Fig. 6. (a) Freundlich and (b) BET isotherm models.

3.3. Isosteric heat of adsorption

Calculations of the isosteric heat of adsorption, denoted by the symbol ΔHs, were performed using the Clausius-Clapeyron equation[24] (Eq.2).

$$\ln(p) = -\frac{\Delta H_S}{RT} + C \tag{2}$$

where p (kpa) is the pressure at which water vapour is fed into the system, The gas constant and temperature are denoted by R and T, respectively, while the integration constant is denoted by C. Initially, by graphing ln(p) vs 1/T, isotherms were converted into isosteres (Figure. 7a) for specific values of the water vapours adsorbed, allowing for the measurement of ΔHs. In order to determine the isosteric heat of adsorption (ΔHs), the slope (-ΔHs/R) was used. Values of ΔHs and correlation coefficients are listed in Table.2, and graphs of the Clausius-Clapeyron equation depicting ΔHs at various adsorption capacities are given in Figure. 7b. Due to the fact that at lower humidity levels, the water molecules were strongly bound to the surface functional groups of the NTPM and mostly manifested as bounded water, it was discovered that Hs values were comparatively greater at lower adsorption capacities.

Table 2. Values of ΔHs and correlation coefficients.

qads	-ΔH_s/R, K	ΔH_s, KJ/mol	R2
0.1	-6.48	53.86	0.988
0.125	-6.078	51.05	0.999
0.15	-5.998	50.43	0.987
0.175	-5.823	49.08	0.992
0.2	-5.819	48.71	0.999
0.225	-5.721	47.92	0.991
0.25	-5.694	47.37	0.999

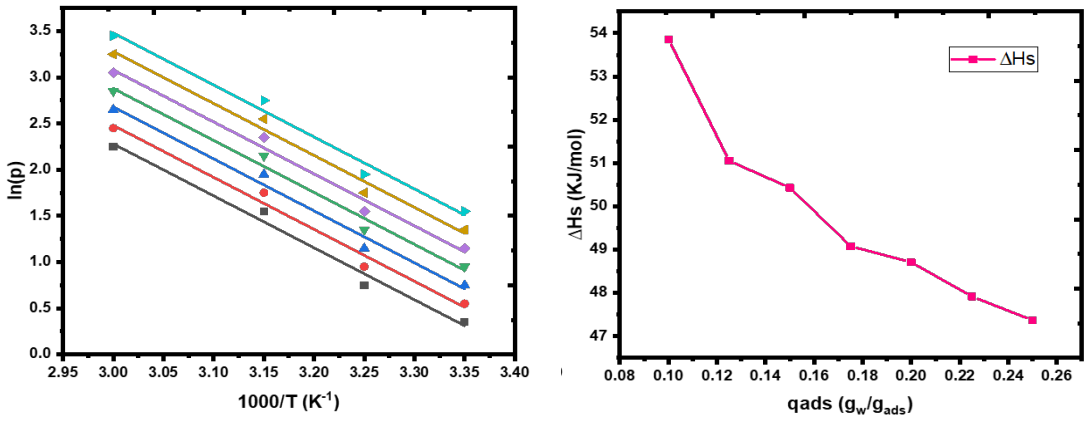

Fig. 7. (a) ln(p) Vs 1/T & (b) the water vapours' isosteric heat of adsorption on NTPM.

Although the partial pressure of water molecules increased as the relative humidity increased and they started penetrating deeper into the internal structure of the adsorbent, the values of ΔHs were relatively modest because the bulk of the water molecules were present as free molecules [25]. NTPM has ΔHs values ranging from 47 to 54 kg/mol (Table 2). At high adsorption capacities, the NTPM's ΔHs value was comparable to water's (44 kJ/mol), indicating that water clusters started to form and eventually filled the pores of the adsorbent with water molecules.[26].

3.4. Kinetics of adsorption

Water vapour adsorption kinetics onto NTPM was investigated at 85% RH (Figure. 8a). Adsorption of water vapours at this relative humidity was first weak, then accelerated for a period, and is again slow as it approaches equilibrium. It's possible that NTPM's initially modest adsorption rate was due to the fact that the membrane polymer's pores were relatively small and the surface was rough. The rate of water vapour adsorption, however, accelerated once the membrane pores opened and began absorbing water molecules through the capillary condensation process[27].

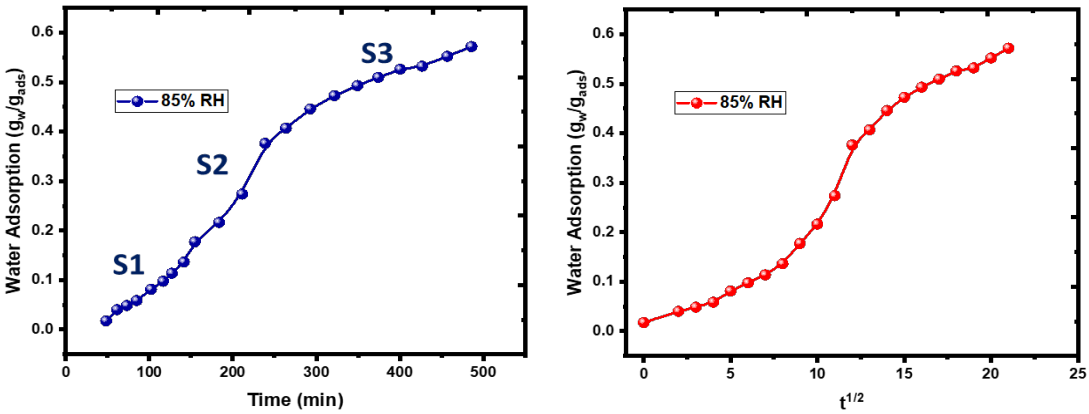

Fig. 8. (a) Adsorption kinetics and (b) NTPM intraparticle diffusion model.

Additionally, when equilibrium was neared, the adsorption of water vapours decreased since the majority of the membrane's polymer structure's holes were now filled with water molecules and new molecules found it difficult to enter the structure. Water molecules condense on the membrane's outer boundary layer to start the multi-step process of adsorption of water vapours on polymer membranes, which is followed by membrane capillary condensation. The pace of adsorption is controlled by the slowest component of the process. Thus, the intraparticle

diffusion (Figure. 8b) model was fitted to experimental kinetics data to identify the rate-controlling step. Model for intraparticle diffusion may be written as[28].

$$q_t = K_{intra\ diffusion} t^{1/2} + \mathrm{C} \quad (3)$$

where adsorption capacity at time t is denoted by q_t. The model's plot should be level and it should
go through the origin if intraparticle diffusion was the sole factor affecting adsorption rate[29]. However, the intraparticle model plot showed that there were really three separate regions (S1, S2, and S3) with their own unique slopes. Consequently, the diffusion process was not only controlled by intraparticle diffusion; other mechanisms may have also contributed. Table 4 summarises the results of the intraparticle diffusion model used to compute the kinetics parameters for sections S1, S2, and S3.

3.5. Reusability and regeneration

Any adsorbent material's effectiveness as a whole is dependent on more than just its adsorption capacity, however; its recyclability and capability for reuse in subsequent adsorption or desorption cycles are also crucial. Therefore, fifteen consecutive adsorption/desorption cycles were conducted to see whether NTPM could be reused. At first, NTPM was subjected to adsorption of water vapours at 85% relative humidity; after equilibrium adsorption condition was reached, the completely hydrated NTPM was regenerated at 60°C and put to use again. Two identical NTPM samples were used to repeat the recycling tests shown in Figure. 9. For the first 10 adsorption cycles, there was no sign of adsorption capacity degradation in the initial sample. Nonetheless, the second sample maintained its adsorption capability during the first nine cycles. Both samples showed excellent reuse efficiency in the fifteenth cycle, at 97% for the first sample and 96% for the second. Over time, mechanical degradation of the polymer structure used in NTPM led to a slight decrease in its adsorption efficiency[30].

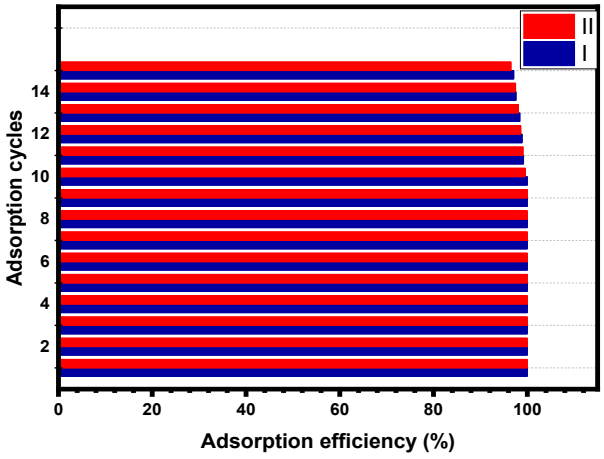

Fig. 9. Repeat the recycling tests for NTPM samples.

4. Conclusion

The NTPM was successfully produced by dispersing nano TiO_2 in polypropylene matrix using CO_2 as blowing agent. The excellent adsorption capacity and quick kinetics were validated by SEM images showing linked capillary channels of pores. In order to extract moisture from damp air, the synthesised NTPM were put to use as solid polymer desiccant materials. When tested at 25 °C and 85% RH, NTPM showed the maximum adsorption capacity of 0.578 gw/gads. The experimental findings were in good agreement with the BET isotherm model, and the

adsorption isotherm fit the type-III isotherm. The findings suggested that the presence of linked capillary channels of pores was the primary reason for its high adsorption capacity. The ability of NTPM to adsorb water decreased as temperature increased, indicating that this process was endothermic. The majority of the water molecules were discovered to be adsorbing via the capillary condensation process and existing as free water molecules in the cavities of NTPM at high humidity levels, as the isosteric heat of adsorption decreased as the adsorption capacity increased. Based on the adsorption kinetics, the type-II diffusion process was hypothesised to be how water molecules entered the polymer structure. The excellent cyclability of NTPM was further demonstrated by fifteen successive adsorption/desorption cycles. This means that a large amount of water can be absorbed by the synthesised solid desiccant material of NTPM without the need for additional hygroscopic materials like deliquescent salts, zeolites, clays, and silica gel. It also means that it has an extraordinarily high capacity to adsorb water vapours.

Acknowledgments

This work was supported by the Noorul Islam Centre for Higher Education, Kumarcoil - 629180, Tamilnadu, India

References

[1] S. Obeid, Y. Al Horr, A. Hakki, and K. N. Abdalla, “A Physicochemical Study of Cost-Effective Liquid Desiccants for Use in an air conditioning system,” University Of Khartoum Engineering Journal, vol. 10, no. 2, 2020. https://doi.org/10.53332/kuej.v10i2.941
[2] K. Murthy, R. J. Shetty, and S. Kumar, “Experimental Analysis and Parametric Study on the Dehumidification System Using Liquid Hybrid Desiccants-A Source of Sustainable Energy,” International Journal of Air-Conditioning and Refrigeration, vol. 29, no. 04, p. 2150038, 2021. https://doi.org/10.1142/S2010132521500383
[3] M. S. A. Ramli et al., “Review of Desiccant in the Drying and Air-Conditioning Application,” Journal homepage: http://iieta. org/journals/ijht, vol. 39, no. 5, pp. 1475–1482, 2021. https://doi.org/10.18280/ijht.390509
[4] X. Chen, S. Riffat, H. Bai, X. Zheng, and D. Reay, “Recent progress in liquid desiccant dehumidification and air-conditioning: A review,” Energy and Built Environment, vol. 1, no. 1, pp. 106–130, 2020. https://doi.org/10.1016/j.enbenv.2019.09.001
[5] M. G. Gado, M. Nasser, A. A. Hassan, and H. Hassan, “Adsorption-based atmospheric water harvesting powered by solar energy: Comprehensive review on desiccant materials and systems,” Process Safety and Environmental Protection, vol. 160, pp. 166–183, 2022. https://doi.org/10.1016/j.psep.2022.01.061
[6] H. Mittal, A. Al-Alili, and S. M. Alhassan, “Adsorption isotherm and kinetics of water vapor adsorption using novel super-porous hydrogel composites,” in Energy Sustainability, 2020, vol. 83631, p. V001T04A003. https://doi.org/10.1115/ES2020-1642
[7] Y. Guo, W. Guan, C. Lei, H. Lu, W. Shi, and G. Yu, “Scalable super hygroscopic polymer films for sustainable moisture harvesting in arid environments,” Nature communications, vol. 13, no. 1, pp. 1–7, 2022. https://doi.org/10.1038/s41467-022-30505-2
[8] Y. Luo et al., “Porous carbon foam based on coassembled graphene and adenine-polyimide for electromagnetic interference shielding,” Polymer, vol. 236, p. 124328, 2021. https://doi.org/10.1016/j.polymer.2021.124328
[9] W. Liang, Y. Hu, X. Zhou, Y. Pan, I. Kevin, and K. Wang, “Variational few-shot learning for microservice-oriented intrusion detection in distributed industrial IoT,” IEEE Transactions on Industrial Informatics, vol. 18, no. 8, pp. 5087–5095, 2021.
[10] M. Aghvami-Panah et al., “A comparison study on polymeric nanocomposite foams with various carbon nanoparticles: adjusting radiation time and effect on electrical behavior and microcellular structure,” International Journal of Smart and Nano Materials, pp. 1–25, 2022. https://doi.org/10.1080/19475411.2022.2107110

[11] M. Hamidinejad et al., "Electrically and thermally graded microcellular polymer/graphene nanoplatelet composite foams and their EMI shielding properties," Carbon, vol. 187, pp. 153–164, 2022. https://doi.org/10.1016/j.carbon.2021.10.075
[12] V. Chaudhary, P. K. Bajpai, and S. Maheshwari, "Effect of moisture absorption on the mechanical performance of natural fiber reinforced woven hybrid bio-composites," Journal of Natural Fibers, 2018. https://doi.org/10.1080/15440478.2018.1469451
[13] K. Rajesh, V. Crasta, N. B. Rithin Kumar, G. Shetty, and P. D. Rekha, "Structural, optical, mechanical and dielectric properties of titanium dioxide doped PVA/PVP nanocomposite," Journal of Polymer Research, vol. 26, no. 4, pp. 1–10, 2019. https://doi.org/10.1007/s10965-019-1762-0
[14] M. Jesus, A. M. Ferreira, L. F. S. Lima, G. F. Batista, R. V. Mambrini, and N. D. S. Mohallem, "Micro-mesoporous TiO_2/SiO_2 nanocomposites: Sol-gel synthesis, characterization, and enhanced photodegradation of quinoline," Ceramics International, vol. 47, no. 17, pp. 23844–23850, 2021. https://doi.org/10.1016/j.ceramint.2021.05.092
[15] M. M. Abutalib and A. Rajeh, "Enhanced structural, electrical, mechanical properties and antibacterial activity of Cs/PEO doped mixed nanoparticles (Ag/TiO_2) for food packaging applications," Polymer Testing, vol. 93, p. 107013, 2021. https://doi.org/10.1016/j.polymertesting.2020.107013
[16] S. Hu et al., "Surface-modification effect of MgO nanoparticles on the electrical properties of polypropylene nanocomposite," High Voltage, vol. 5, no. 3, pp. 249–255, 2020. https://doi.org/10.1049/hve.2019.0159
[17] M. A. Morsi, A. H. Oraby, A. G. Elshahawy, and R. M. Abd El-Hady, "Preparation, structural analysis, morphological investigation and electrical properties of gold nanoparticles filled polyvinyl alcohol/carboxymethyl cellulose blend," Journal of materials research and technology, vol. 8, no. 6, pp. 5996–6010, 2019. https://doi.org/10.1016/j.jmrt.2019.09.074
[18] R. Bardestani, G. S. Patience, and S. Kaliaguine, "Experimental methods in chemical engineering: specific surface area and pore size distribution measurements—BET, BJH, and DFT," The Canadian Journal of Chemical Engineering, vol. 97, no. 11, pp. 2781–2791, 2019. https://doi.org/10.1002/cjce.23632
[19] Jeevanantham V, Tamilselvi D, Rathidevi K and Bavaji SR, P Neelakandan, Biomass Conversion and Biorefinery, 1-10, https://doi.org/10.1007/s13399-023-04179-9
[20] H. Mittal, A. Al Alili, and S. M. Alhassan, "Hybrid super-porous hydrogel composites with high water vapor adsorption capacity–Adsorption isotherm and kinetics studies," Journal of Environmental Chemical Engineering, vol. 9, no. 6, p. 106611, 2021. https://doi.org/10.1016/j.jece.2021.106611
[21] X. Zhou, H. Lu, F. Zhao, and G. Yu, "Atmospheric water harvesting: a review of material and structural designs," ACS Materials Letters, vol. 2, no. 7, pp. 671–684, 2020. https://doi.org/10.1021/acsmaterialslett.0c00130
[22] J. Wang et al., "High-yield and scalable water harvesting of honeycomb hygroscopic polymer driven by natural sunlight," Cell Reports Physical Science, vol. 3, no. 7, p. 100954, 2022. https://doi.org/10.1016/j.xcrp.2022.100954
[23] F. Deng, Z. Chen, C. Wang, C. Xiang, P. Poredoš, and R. Wang, "Hygroscopic Porous Polymer for Sorption-Based Atmospheric Water Harvesting," Advanced Science, p. 2204724, 2022. https://doi.org/10.1002/advs.202204724
[24] N. Pal and M. Agarwal, "Advances in materials process and separation mechanism of the membrane towards hydrogen separation," International Journal of Hydrogen Energy, vol. 46, no. 53, pp. 27062–27087, 2021. https://doi.org/10.1016/j.ijhydene.2021.05.175 https://doi.org/10.1021/acs.jpcc.9b05758
[25] Jeevanantham V, Tamilselvi D, Bavaji SR and Mohan S, Bulletin of Materials Science, 46 (1), 32 (2023); https://doi.org/10.1007/s12034-022-02868-1
[26] S. Ntsondwa, V. Msomi, and M. Basitere, "Evaluation of the Adsorptive Process on Adsorbent Surfaces as a Function of Pressure in an Isosteric System Compared with Adsorption Isotherm," ChemEngineering, vol. 6, no. 4, p. 52, 2022. https://doi.org/10.3390/chemengineering6040052

[27] G. Rother, A. G. Stack, S. Gautam, T. Liu, D. R. Cole, and A. Busch, “Water uptake by silica nanopores: impacts of surface hydrophilicity and pore size,” The Journal of Physical Chemistry C, vol. 124, no. 28, pp. 15188–15194, 2020. https://doi.org/10.1021/acs.jpcc.0c02595
[28] J. Bai et al., “Impact of surface chemistry and pore structure on water vapor adsorption behavior in gas shale,” Chemical Engineering Journal, vol. 402, p. 126238, 2020. https://doi.org/10.1016/j.cej.2020.126238
[29] Y. Byun, S. H. Je, S. N. Talapaneni, and A. Coskun, “Advances in porous organic polymers for efficient water capture,” Chemistry–A European Journal, vol. 25, no. 44, pp. 10262–10283, 2019. https://doi.org/10.1002/chem.201900940
[30] Jeevanantham V, Tamilselvi D, Rathidevi K and Bavaji SR, Journal of Materials Research 38 (7), 1909-1918 https://doi.org/10.1557/s43578-023-00965-3